Atmos. Chem. Phys. Discuss., 13, 7463–7502, 2013
www.atmos-chem-phys-discuss.net/13/7463/2013/
doi:10.5194/acpd-13-7463-2013

Atmospheric Chemistry and Physics Discussions
Open Access

Secondary aerosol formation from stress-induced biogenic emissions and possible climate feedbacks

Th. F. Mentel[1], E. Kleist[2], S. Andres[1], M. D. Maso[1,3,*], T. Hohaus[1], A. Kiendler-Scharr[1], Y. Rudich[4], M. Springer[1], R. Tillmann[1], R. Uerlings[2], A. Wahner[1], and J. Wildt[2]

[1]Institut für Energie und Klimaforschung, IEK-8, Forschungszentrum Jülich, Germany
[2]Institut für Bio- und Geowissenschaften, IBG-2, Forschungszentrum Jülich, Germany
[3]Department of Physics, University of Helsinki, P.O. Box 48, 00014, Helsinki, Finland
[4]Weizmann Institute of Science, Rehovot, 76100 Israel
[*]now at: Dept. of Physics, Tampere University of Technology, 33101 Tampere, Finland

Received: 2 February 2013 – Accepted: 5 March 2013 – Published: 20 March 2013

Correspondence to: Th. F. Mentel (t.mentel@fz-juelich.de)

Published by Copernicus Publications on behalf of the European Geosciences Union.

Abstract

Atmospheric aerosols impact climate by scattering and absorbing solar radiation and by acting as ice and cloud condensation nuclei. Secondary organic aerosols (SOA) comprise an important component of atmospheric aerosols. Biogenic volatile organic compounds (BVOC) emitted by vegetation are a major source of SOA. Pathogens and insect attacks, heat waves and droughts can induce stress to plants that may impact their BVOC emissions, and hence the yield and type of formed SOA, and possibly their climatic effects. This raises questions whether stress-induced changes in SOA formation may attenuate or amplify effects of climate change. In this study we assess the potential impact of stress-induced BVOC emissions on SOA formation for tree species typical for mixed deciduous and Boreal Eurasian forests. We studied the photochemical SOA formation for infested plants in a laboratory setup under well-controlled conditions and applied in addition heat and drought stress. The results indicate that stress conditions substantially modify SOA formation. While sesquiterpenes, methyl salicylate, and C_{17}-BVOC increase SOA yield, green leaf volatiles suppress SOA formation. By classifying emission types, stressors and SOA formation potential, we propose possible climatic feedbacks regarding aerosol effects. We conclude that stress situations for plants due to climate change should be considered in climate-vegetation feedback mechanisms.

1 Introduction

Terrestrial vegetation is a key player in the biogeochemical cycles of carbon and water and thus a key player for Earth's climate (Carslaw et al., 2010). In addition vegetation constantly emits reactive biogenic volatile organic compounds (BVOC) to the atmosphere where they participate in atmospheric gas-phase chemistry and particle formation. On a global scale, BVOC emissions exceed anthropogenic VOC emissions by an order of magnitude (Guenther et al., 1995, 2012). BVOC play an important role in atmospheric oxidation cycles; they affect ozone formation, the oxidation capacity of the atmosphere, and they are important players in new particle formation (Riipinen et al., 2011). BVOC oxidation products generate biogenic secondary organic aerosols (BSOA) and increase the number and size of aerosol particles, as shown by Tunved et al. (2006) for monoterpenes (MT). Both attributes are significant with respect to the direct and the indirect effects of aerosols on the radiation budget of the Earth via scattering, absorption of sun light and through modification of cloud properties (Tunved et al., 2008; Kerminen et al., 2005; Spracklen et al., 2008; Heald et al., 2008). Kulmala et al. (2004) and Goldstein et al. (2009) proposed that the increase in BSOA burden would cause a negative climate feedback through scattering of incoming solar radiation between the terrestrial ecosystem and the atmosphere, attenuating the temperature increase expected due to climate warming.

Climatic changes will alter the environmental conditions for vegetation (Sitch et al., 2007). Vegetation models predict that under future global climatic changes, forests in Temperate and Boreal regions will flourish and spread, suggesting that this expansion will increase the annual global production of BVOC and BSOA (Lathière et al., 2005; Tsigaridis and Kanakidou, 2007). Climate models also predict frequent heat waves as well as changes in precipitation (Trenberth et al., 2007). It is noted that predictions of future BVOC emissions assume equilibrium between vegetation and climate (Lathière et al., 2005). However, noticeable climate change will appear already within the next decades whereas vegetation propagates by only several tens of kilometers in 100 yr (Chen et al., 2011). Thus the time scale of substantial climatic changes may be short compared to typical adaptation times of vegetation.

We thus hypothesize that vegetation in many regions will be forced out of the optimal living conditions as the plants will be exposed to more heat waves, dryness, pollution, insect outbreaks or various diseases due to climate change (Arneth et al., 2010). It is projected that such deviations will disturb the functioning of plants, denominated as stress to the plants. Our recent experiments suggest that it may not be sufficient to consider only isoprene and MT (Kleist et al., 2012) and BSOA originating from those compounds in future (and current) climate scenarios.

Phenomenological algorithms of BVOC emissions consider temperature and light intensity as the driving factors for the emission strengths of MT and isoprene (e.g. Guenther et al., 1993; Schuh et al., 1997; Kesselmeier and Staudt, 1999), but omit BVOC emissions in response to other stresses on plants (Heiden et al., 1999, 2003; Arneth and Niinemets, 2010; Peñuelas and Staudt, 2010; Loreto and Schnitzler, 2010). The latter emissions are termed stress-induced emissions (SIE). SIE are transient as they only appear during or after stress impacts. They consist of different BVOC classes such as green leaf volatiles (GLV, e.g. Croft et al., 1993) or phenolic BVOC (e.g. Heiden et al., 1999; Colquhoun et al., 2010; Guenther et al., 2012). Furthermore MT, homo-, and sesquiterpenes (SQT) are emitted as plant's response to pathogen or herbivore attacks (e.g. Hopke et al., 1994; Boland et al., 1995). Upon atmospheric oxidation, SIE may contribute significantly to BSOA formation similar to the constitutive emissions (Joutsensaari et al., 2005). Enhanced BSOA number formation during winter-spring transition stress has also been observed in the field (Dal Maso et al., 2009).

Recently, we studied the effect of heat stress on constitutive emissions and SIE in terms of *de novo* emissions and emissions from storage pools (Kleist et al., 2012). Here we survey which SIE contribute to BSOA formation and to what extent. To assess BSOA formation from SIE we performed experiments with real plants in the Jülich Plant – Atmosphere Chamber (JPAC). The plants were exposed to biotic stressors and were in addition exposed to heat and drought stress in order to characterize the impact of abiotic stressors on SOA formation.

The emitted BVOCs reacted with OH and ozone and the resulting SOA mass was determined. We term the first derivative of the SOA mass as a function of the chemical consumption of the BVOC mass as the incremental mass yield or as the SOA formation potential of a BVOC mix. The incremental yield quantifies the efficiency to convert BVOC mass by gas-phase oxidation into particulate matter.

2 Experimental

Experiments were conducted in the Jülich Plant – Atmosphere Chamber facility (JPAC). A detailed description of the chamber set up and its performance is given in Mentel et al. (2009). In short, the facility consists of three Borosilicate glass chambers (164 L, 1150 L, and 1450 L) with Teflon floors. Each chamber is mounted in separate climate controlled housing (adjustable between 10 and 50 °C). Either one of the two smaller chambers was used as plant chamber. The large chamber was used as reaction chamber for studying SOA formation. Discharge lamps (HQI 400 W/D; Osram, Munich, Germany) simulated the solar light spectrum. At full illumination the photosynthetic photon flux density (PPFD) was 480 $\mu mol\,m^{-2}\,s^{-1}$ in the 1150 L chamber and 800 $\mu mol\,m^{-2}\,s^{-1}$ in the 164 L chamber.

Clean air was pumped through the plant chamber to take up BVOC emitted by the plants. A fraction of the air leaving the plant chamber ($\approx 16\,L\,min^{-1}$) was fed into the reaction chamber. The reaction chamber had a separate inflow of $\approx 16\,L\,min^{-1}$ to add ozone and humidified air. The conditions in the reaction chamber were held constant for all experiments ($T = 17 \pm 0.5\,^{\circ}C$, $RH = 63 \pm 2\,\%$, $[O_3] = 85$–90 ppb without UV light). OH radicals were generated by ozone photolysis (internal UV lamp, Philips, TUV 40 W, $\lambda_{max} = 254$ nm, $J(O^1D) \approx 2.9 \times 10^{-3}\,s^{-1}$) and subsequent reaction of O^1D with water. OH radicals were generated when the BVOC concentrations in the reaction chamber had reached a steady state. OH radical concentrations ranged from 10^7 to $10^8\,cm^{-3}$. The presence of OH radicals induced new particle formation. Particle concentration (particle diameter $d_p > 7$ nm) and size distribution (15 nm $< d_p <$ 700 nm) were measured by a condensation particle counter (CPC TSI3022A) and a Scanning Mobility Particle Sizer (SMPS TSI3071 + TSI3025A), respectively. We were allowing 8 h for establishing a new steady state in the reaction chamber for the next experiment after conditions in the plant chamber were changed.

Varying the conditions in the plant chamber enabled determining the impact of a varying BVOC load and BVOC patterns on SOA formation and yield. BVOC concentrations were measured at the outlet air of the plant chamber and the reaction chamber using GC-MS (Heiden et al., 1999). OH concentrations were determined by the decrease of deuterated cyclohexane (C_6D_{10}) added to the reaction chamber (Kiendler-Scharr et al., 2009). Calibration of the GC-MS was conducted as described in Heiden et al. (2003). To calibrate the C_{17}-BVOC emitted from insect infested spruce we used 8-heptadecene (Fluka, GC purity) as a surrogate for emitted C_{17}-compounds.

We performed five experiments – three with plants and two control experiments. These experiments are summarized in Table 1. For the experiments 1, 2, and 3 with plants we used three to four years old seedlings of spruce (*Picea abies* L.), pine (*Pinus sylvestris* L.), beech (*Fagus sylvatica* L.), and birch (*Betula pendula* L.). The plants were stored near a natural forest before the measurements to obtain realistic conditions with all the impacts that plants experience in their natural environment. The plants suffered from typical diseases as insect or pathogen attacks and featured SIE when they were introduced into the plant chamber. Up to four plants were introduced together into the plant chamber (see Table 1).

In Experiment #1 we used seedlings of one silver birch (*Betula pendula* L.), one Scots pine (*Pinus sylvestris* L.), and one Norway spruce (*Picea abies* L.) together as BVOC source. The spruce showed a high degree of aphid infestation. No infestation was visible for the other trees, but they also may have been infested. The plants were introduced into the 1150 L plant chamber, acclimated for one day and investigated over 18 days. A diurnal cycle of light was applied: 13 h illumination, 9 h darkness and simulations of twilight for 1 h in the morning and evening respectively. The light intensity (PPFD) was normally set to 480 μmol m^{-2} s^{-1} during the periods of illumination. To vary the emission strength, the plant chambers temperature was set either to 15 or 20 °C at different days. PPFD was varied from day to day in steps of 120 μmol m^{-2} s^{-1} at $T = 15$ °C on several occasions.

In Experiment #2 we investigated an individual Norway spruce severely infested by aphids. This plant was investigated for 11 days in total. During the first five days, moderate temperatures were applied to the plant (days –5 to –1, $T = 15$ or 20 °C), Table 2).

Higher temperatures of 35 °C and 30 °C were applied on day 0 and day 1, respectively. During the remaining 4 days, moderate temperatures of 20 °C were applied (days 2 to 5). During the entire measurement period the diurnal light cycle was the same with PPFD = 480/0 µmol m^{-2} s^{-1} during periods of illumination/darkness. Table 2 lists the temperatures together with the measured MT/SQT ratios ([µg m^{-3}]/[µg m^{-3}]).

In Experiment #3 we used a set of four trees typical for the central European mixed forest (one spruce, one birch and two beech seedlings). The spruce was infested by the aphid *Cinara Pilicornis* and emitted long chained C_{17}-alkenes. The birch did not show visible symptoms of injury but both beech seedlings showed symptoms of drought stress visible by leaf curling. We did not irrigate the soil for 5 days in order to apply drought stress in addition to the infestation. The diurnal light cycle was: PPFD = 480/0 µmol m^{-2} s^{-1} during periods of illumination/darkness. Plant chamber temperature was held constant at 20 °C, except for the last day when it was increased to 25 °C.

For the control Experiments #1c and #3c the substances were evaporated from diffusion sources, diluted by synthetic air and continuously flushed into the reaction chamber. As for plant emissions SOA formation was induced by ozone photolysis in presence of water and subsequent OH formation. UV light was switched on and particle formation was induced when steady state concentrations were reached after three hours.

In control Experiment #1c we determined the impact of methyl salicylate (MeSa) on BSOA formation. We added MeSa, deuterated cyclohexane-d10 and α-pinene to the reaction chamber. Concentrations of α-pinene and cyclohexane were held constant and the steady state concentration of α-pinene would have been 27 ± 3 µg m^{-3} (4.8 ± 0.6 ppb) if ozone reactions were absent; cyclohexane-d10 concentrations were 1.5 µg m^{-3} (∼ 0.4 ppb). MeSa concentrations were varied between 0 and 55 µg m^{-3} (0 to 8.8 ppb). SOA formation was induced by oxidation of the reaction mix by OH radicals ([OH] $\sim 6\times10^7$ cm^{-3} (see Fig. 3), [O_3] 40–50 ppb with UV light switched on and [O_3] = 85–90 ppb with UV light switched off, reaction chamber temperature 17 ± 0.5 °C, RH = 63 ± 2 %). OH concentrations were determined from the difference of cyclohexane-d10 concentrations at chamber outlet with and without the UV light. Less than 60 % of the added MeSa reacted with OH radicals due to the low reactivity of MeSa.

In control Experiment #3c we investigated the drastic effect of GLV observed in the experiment #3 induced by drought stress. Again we added α-pinene ($43 \pm 4\,\mu g\,m^{-3}$) to the reaction chamber and d_{10}-cyclohexane to trace OH concentrations. As a typical GLV we added (Z)-3-hexenol to the reaction chamber in varying concentrations at otherwise unchanged conditions. Experiments were conducted from day to day with (Z)-3-hexenol concentrations varying from 0 to $48\,\mu g\,m^{-3}$. SOA formation was induced by oxidation of α-pinene by OH ($[OH] \sim 6 \times 10^7$–$1.6 \times 10^7\,cm^{-3}$, $[O_3] = 85$–90 ppb in absence and 40–50 ppb in the presence of UV light, respectively, $T = 17 \pm 0.5\,^{\circ}C$, RH = 63 ± 2 %).

For the determination of incremental mass yields one needs to know the amount of chemically consumed BVOC. This quantity was directly obtained by comparing the concentrations of the reactants entering and leaving the reaction chamber. Generally, more than 98 % of the MT and SQT entering the reaction chamber were oxidized at the typical OH and O_3 concentrations in the reaction chamber. In these cases the chemical consumption was set equal to the input amount. For MeSa, which reacted to less than 60 %, the chemical consumption was calculated from the difference of MeSa concentrations with and without UV light switched on.

Maximum SOA mass was reached after 1–2 h, depending on the concentrations of BVOC and oxidants. The observed maximal particle mass was corrected for the loss by outflow and plotted versus the BVOC consumption in the reaction chamber as described in Mentel et al. (2009). As the basis for BVOC consumption we used the mass (in $\mu g\,m^{-3}$) summed up over all detected BVOC, independent of their biosynthetic origin.

It has to be noted that uncertainties for the yields given here were determined from statistical errors only. Possible systematic errors such as erroneous calibration (GC-MS data: ±15 % for MT and ±20 % for SQT) were not included. All measurements were performed under low NO_x conditions (NO_x < 300 ppt).

3 Results

Experiment #1 SOA formation from sesquiterpenes and methyl salicylate

Under the conditions of Experiment #1, the plants emitted mainly SQT and phenolic BVOC, indicating that the main portion of the emissions was induced by biotic stress, most probably due to the insect infestation. Considering that there was no active control on the stress impacts imposed by the insect infestation, both, emission strengths as well as the emission patterns were fairly stable for constant temperature and constant PPFD (Fig. 1A). The ratios SQT/MT and phenolic/MT covered ranges of 4.1–5.8 (average = 4.8 ± 0.8) and 3.2–5.6 (average = 3.8 ± 1.0), respectively. Variation of temperature changed essentially only the emission strengths. SQT and phenolic BVOC are *de novo* emissions and the emission strengths also depend on PPFD (Fig. 1b, Kleist et al., 2012). This observation is in agreement with the results by Gouinguene and Turlings (2002). For $120 \leq \text{PPFD} \leq 480\,\mu\text{mol}\,\text{m}^{-2}\,\text{s}^{-1}$ SQT/MT and phenolic/MT varied from 9–21 and 6–9, respectively.

For the infested plants in Experiment #1, SQT contributed up to 56 % to the total emissions and phenolic BVOC up to 44 %. MT (≤ 10 %) and GLV (≤ 1 %) were only minor fractions of the mix of reactive BVOC. Main abundant SQT were α-farnesene (~ 27 %) and β-farnesene (~ 66 %). About 95 % of the phenolic BVOC was MeSa. Other phenolic BVOC that were emitted in minor amounts were compounds such as methyl benzoate (~ 1 %) or benzyl benzoate (~ 0.7 %). Table 3 lists the BVOC found in the emission mix, their concentrations and their contribution to the total VOC emissions from this set of plants.

SOA formation was observed only in the presence of OH as for unstressed plants (Mentel et al., 2009). Ozonolysis alone did not lead to SOA formation. A 22 ± 2 % incremental SOA mass yield was determined for this mixture from the slope of linear fit in Fig. 2 (Fig. 2). This incremental yield is significantly higher than the 4–6 % value measured for a mixture consisting of MT only (Mentel et al., 2009; Lang-Yona et al., 2010), but is similar to that obtained for stressed transgenic poplar plants (Kiendler-Scharr et al., 2012) that exhibited a similar emission pattern as the plants used here. The positive x-intercept in Fig. 2 and in similar plots in the following indicates the nucleation threshold in JPAC (Mentel et al., 2009) and is not further considered here.

It was impossible to identify the contribution of the different BVOC on SOA formation because the plants co-emitted SQT and MeSa. Therefore we determined independently the SOA yield for MeSa in control Experiment #1c using α-pinene and MeSa from artificial sources. The α-pinene is as a representative for constitutive SOA precursors to induce SOA formation. Its concentration was held constant at $25\,\mu g\,m^{-3}$ (4.5 ppb), while MeSa concentrations were varied between 0 and $55\,\mu g\,m^{-3}$ (0 to 8.8 ppb). The incremental mass yield of the α-pinene/MeSa mixture was determined to $20 \pm 3\,\%$ (slope in Fig. 3). Since only MeSa concentrations were varied, the incremental yield is due to MeSa. The OH concentrations were not affected much by the increasing MeSa concentrations due to the low reactivity of MeSa (Fig. 3). The incremental yield for MeSa has the same magnitude as that obtained with the mix of MeSa and SQT emitted from the set of plants in Experiment #1.

Experiment #2: impacts of heat stress on SOA formation

Figure 4 shows the concentrations of different BVOC classes at the inlet of the reaction chamber during Experiment #2 with the infested spruce over 11 days. The emission strengths of SQT and MT decreased over the first 4 days (days −5 to −2 in Table 2 and Fig. 4) and also the emission pattern was not strictly constant. During the first 4 days, SQT emissions were higher than MT emissions. Only on day −1, when the temperature of the plant chamber increased to 25 °C, the MT emissions were somewhat higher than SQT emissions.

When the spruce was exposed to heat stress of $T = 35\,^{\circ}C$ for 9 h on day 0 and $T = 30\,^{\circ}C$ for 10 h on day 1, we observed a strong increase of MT emissions due to a damage of the resin ducts where MT are stored. SQT emissions changed significantly less during the heat stress (compare Kleist et al., 2012).

Following the heat stress, the plant was held at 20 °C for another 4 days (day 2–day 5), during which SQT emissions decreased each day until they reached the instrumental detection limit on day 3. The heat stress had caused decline of SQT. The MT emissions also decreased from day 2 to day 5, possible due to plant internal repair of pool damage.

SOA formation was measured during the whole period of 11 days. For the days −5 to day −2 with MT/SQT ratios of 0.27–0.49 the incremental yield for this BVOC mix containing significant portions of SQT was 17 ± 1 %. With the onset of the heat stress on day 0 the MT emissions increased more than 20 fold while the SQT emissions decreased. As can be seen in Fig. 5 (large red triangle), the increased total emissions at day 0 led to more SOA mass during the heat stress than during the days before. This is only a single observation, however, the data point for day 0 is significantly off the line of the SQT dominated yield curve. Moreover, the MT dominated (days 0, 1, 2) showed an incremental yield of 8.8 ± 0.2 %, $R^2 = 0.96$ (Table 2, red triangles in Fig. 5). This is lower than that before the heat stress and closer to the expected MT-SOA yields of 4–6 % (Mentel et al., 2009; Lang-Yona et al., 2010).

During the period day 2 to day 5 after applying the heat stress, the plant was held at moderate $T = 20$ °C and the MT emissions dropped back to lower amounts but SQT emissions did not recover. The total BVOC emissions were lower than before the heat stress and from day 3 on the MT emissions were so low that formation of particles with $d_p > 7$ nm was not observed at all.

Experiment #3: interaction of C_{17}-BVOC emissions and GLV emissions during drought stress

In experiment #3 with birch, beech, and a spruce infested by *Cinara Pilicornis*, C_{17}-BVOC dominated the BVOC mix exiting the plant chamber contributing to about 60 % to the emission of carbon (MT ~ 30 %, SQT ~ 5 % GLV ~ 2 %). Most abundant C_{17}-compounds were 8-heptadecene, 6,9-heptadecadiene, and 3,6,9-heptadecatriene. On day 0 when the leaves of the beeches showed strong curling due to the continuing drought a strong emission pulse of GLV appeared. As shown in Fig. 6, on day 0 the GLV contributed to nearly 40 % to the emitted carbon whereas the contribution of MT dropped from 25 to 4 % (11 to 3 ppbC). After the strong GLV pulse, the MT remained at a low level (~ 4 %). The contribution of GLV was about 10 % for the next days and decreased to roughly 3 % about a week after the strong pulse. Both, the contribution of the C_{17}-BVOC to the emission pattern as well as the absolute emissions of these compounds increased during the period day 1 to day 8 (Fig. 6).

Figure 7 shows the data obtained for maximum SOA mass during that experiment. With exception of the strong GLV pulse, we observed a good linear relationship between maximum SOA volume and BVOC concentrations with an incremental yield of 33 ± 6 % (black circles in Fig. 7). This yield is even higher than that obtained for the mixtures consisting mainly of SQT (17 ± 1 %), MeSa (20 ± 3 %) and SQT and MeSA (22 ± 2 %). In contrast, the data point obtained at the high GLV contribution to the mixture (green square in Fig. 7, day 0 in Fig. 6) showed a significant deviation from the linear relationship obtained for BVOC dominated by C_{17}-BVOC emission. The mix containing the GLV had obviously a much lower potential for SOA formation than the mix without GLV.

The less efficient particle formation during the GLV emission pulse suggests a counteracting effect of GLV on SOA yield. Therefore we investigated the impact of GLV emissions on SOA formation in reference Experiment #3c with α-pinene as constitutive SOA precursor and (Z)-3-hexenol as surrogate for a GLV. The α-pinene concentration was held constant at 43 ± 4 $\mu g\ m^{-3}$ while (Z)-3-hexenol was added to the chamber in concentrations varying from 0 to 48 $\mu g\,m^{-3}$. The amount of SOA formed from the mixtures of α-pinene and (Z)-3-hexenol as well as the OH concentrations in the reaction chamber decreased with increasing (Z)-3-hexenol addition (Fig. 8). It is clearly seen that with increasing (Z)-3-hexenol addition and consumption the formation of SOA mass and the OH radical concentrations are suppressed (note the logarithmic scale for OH in Fig. 8). The suppressing impact of (Z)-3-hexenol on particle formation may possibly be similar to that of isoprene (Kiendler-Scharr et al., 2009). The data obtained with (Z)-3-hexenol confirmed that the deviation of the data point at high GLV in Experiment #3 (green square in Fig. 7) was due to the suppressing effect of GLV.

In all three experiments with plants, the BVOC were introduced into the reaction chamber together with up to 90 ppb ozone (see Sect. 2). Particle formation ($d_p > 7$ nm) from ozonolysis alone was negligible when BVOC concentrations were below 50 µg m^{-3} (~ 100 ppbC), even in presence of up to 36 % SQT (17 µg m^{-3}). In these experiments BVOC concentrations were more than an order of magnitude higher than those typically observed in the planetary boundary layer. Our observation supports the role of OH for the particle formation process in the atmosphere.

4 Discussion

4.1 SOA formation from constitutive BVOC emissions and SIE

In order to assess the impact of SIE we will refer to previous experiments in the JPAC chamber with unstressed spruce and pine, and *α*-pinene (Mentel et al., 2009). In these cases, MT emissions constituted more than 85 % of the BVOC emissions and OH-initiated SOA formation resulted in linear relationships between consumed BVOC mass and observed SOA mass giving the incremental yields for SOA formation as listed in Table 4 (Mentel et al., 2009). Because of their low contribution to emissions from the unstressed plants, neither SQT, nor phenolic BVOC or isoprene had significant impact on the incremental yields in these experiments. The incremental yields for MT dominated BVOC mixes, including holm oak, were 4 to 6 %, independent of the plant species and independent of the detailed MT emission pattern (Mentel et al., 2009; Lang-Yona et al., 2010). Hao et al. (2011) found SOA mass yields of 3–11 % in experiments with pine and spruce emissions with variable MT pattern, commensurable to our findings, if their higher loads are considered.

From Experiments #1c and #2 we derive incremental mass yields of 20 ± 3 % for MeSa and 17 ± 1 % for SQT, respectively (Table 4). The SQT and MeSa incremental yields are about the same within the errors and we conclude that SQT and MeSa must have contributed according to their turnover to the SOA yields of ≈ 20 % in Experiment #1 (Table 4 and Kiendler-Scharr et al., 2012). Compared to the incremental yields of MT-SOA, the yields of SQT-SOA and MeSa-SOA are about a factor of 4 larger. Therefore we conclude that in biotic stress situations, when plants invest in SQT or in MeSa instead of in MT synthesis more SOA mass (and more SOA particles) can be formed from the same amount of C emitted as BVOC.

Under infestation by aphid *Cinara Pilicornis* causing emissions of C_{17}–BVOC, (Experiment #3) the enhancement of the incremental SOA yield (33 %) is even larger, about a factor of 6 compared to MT. This is attributed to the C_{17}-BVOC. Not much is known with respect to the emissions of the C_{17}-compounds, however, one of the major components, 8-heptadecene, was found by Nazzi et al. (2002) during interactions of the parasitic mite *Varroa destructor* and plant cells indicating that the C_{17}-compounds were indeed of biogenic origin. Measurements with the isolated spruce after Experiment #3 showed that the C_{17}-BVOC originated indeed from the plant that was infested by the aphid *Cinara Pilicornis.* We did not separate out whether these compounds originated from the plant itself or from the insects or the insects' excrements that were visible as small droplets on needles and branches of the plant. However, independent of the detailed emission mechanism, these compounds originate from the coupled plant-insect system and were therefore treated as a stress-induced BVOC class.

The emission of SQT, MeSa, and C_{17}-BVOC in response to biotic stress is known (e.g. Nazzi et al., 2002; Colquhoun et al., 2010; Joó et al., 2011; Kleist et al., 2012). Since these compound classes provide a larger SOA potential per emitted carbon than constitutive MT emissions, particles grow to larger sizes. (In addition more aerosol particles were formed in our experiments.) If the biotic stress to plants occurs as a regional phenomenon, the enhanced aerosol size (and number) will contribute on a regional scale to the direct (Pilinis et al., 1995; Chen et al., 2009; Kaufman et al., 2002) and indirect aerosol effects (Albrecht, 1989; Twomey, 1977; Kaufman et al., 2002; Lohmann and Feichter, 2005; Quaas et al., 2009) on climate.

SIE-SOA will provide extra growth and thus potentially stronger scattering compared to the same turnover of constitutive MT amount. A similar argument holds for the first indirect effect (Twomey effect): to become CCN-active, particles must grow to several tens of nm or even more. Provided that SIE-SOA are as good CCN as MT-SOA, they will add extra growth and formation of more CCN, which could lead to more and smaller cloud droplets (for a given amount of available water) thus to more reflective clouds. Both direct and first indirect effect eventually exert a cooling effect which counteracts warming, thus constituting an overall negative feedback if the plant stress was favored or caused by heat.

The increase of the cloud droplet number which increases the cloud albedo also prolongates the cloud lifetime by suppression of rain (second indirect effects). If the plant stress that induced GLV emissions is caused or favored by drought periods, suppression of SOA formation by GLV emissions can decrease the cloud droplet number and increase rain probability. This behavior could also provide a negative feedback.

The discussion above considered only the higher SOA *potential* of SQT and MeSa which is an important prerequisite for a more effective SOA formation. The eventual effect does not only depend on the SOA potential but also on the emitted *amounts* of BVOC and their turnover in the atmosphere. In a situation of long periods with increased SIE as depicted in Fig. 1 and Fig. 6, the situation is straightforward and will lead to aerosol effects as sketched above. However, if stress causes plant damage as shown in Experiment #2 (Fig. 4), the SOA production may die out to zero after a short pulse.

The situation becomes more complex if one considers the GLV that were triggered by drought stress. Although GLV itself have some limited mass yield of 3 % for (Z)-3-hexenol (Hamilton et al., 2009), they can hinder SOA formation from constitutive emissions such as α-pinene (Experiment #3c) or diminish the SOA potential even of the very effective SIE of C_{17}-BVOC (green data point in Fig. 7). This effect of GLV goes along with a drop in OH radical concentration (Fig. 8), in contrast to the effect of MeSa (Fig. 3). The GLV effect shows similarity to the suppressing effect of isoprene (Kiendler-

Scharr et al., 2009, 2012), where the reactive isoprene with a limited SOA mass yield of a few percent prevents nucleation and SOA formation from constitutive MT emission and SIE, respectively. While climate warming could enhance the isoprene to MT ratio steadily, the GLV effect would become active episodically whenever plants are damaged in cases such as drought stress. This may lead to a positive feedback namely, drought → GLV → less OH → less SOA → increasing heat → extended drought.

4.2 Climate change and SIE-SOA

Although we quantified SOA formation potentials for various SIE, the difficulty to quantify stressors and their impacts impedes *quantitative* upscaling of our results at the current stage. A major uncertainty is also the future evolution of biotic stressors like pathogen and insect attacks. The effect of climate change on pathogens and herbivoric insects depends on the detailed conditions of the eco-systems. However, there is evidence that biotic stress will increase together with heat waves and droughts (e.g. Ayres and Lombardero, 2000; Arneth and Niinemets, 2010; Bentz et al., 2010; Hicke et al., 2012; Sturrock et al., 2011). We will try to point out possible future trends in Temperate and Boreal regions considering the *aerosol effects* of constitutive MT-SOA and SIE-SOA based on the formation potentials in Table 4 and discuss possible implications of SIE with respect to climate change.

Table 5 sketches expected effects of BVOC emissions on SOA formation based on the measurements presented here. Furthermore possible responses of constitutive emissions and SIE to biotic stress and to heat and drought are outlined. Beside classification into constitutive and stress-induced emissions, we also took into account the basic emission mechanisms as BVOC emissions may either be *de novo* emissions or arise from storage in plant organs. The impacts of stress vary with the emission mechanisms. For example, heat or drought can strongly suppress overall biosynthetic activity. Coherently, *de novo* MT emissions will tend to decrease. However, under heat stress MT emissions from plant internal pools can still increase on time scales of days to weeks (e.g. Kleist et al., 2012).

Title Page
Abstract | Introduction
Conclusions | References
Tables | Figures
◀| |▶
◀ ▶
Back | Close
Full Screen / Esc
Printer-friendly Version
Interactive Discussion

The base cases are constitutive MT emissions. Incremental yields of MT are independent of the detailed MT mix and the amount of produced particle mass predominantly depends on the *amount* of emitted MT (Mentel et al., 2009; Lang-Yona et al., 2010; Hao et al., 2011). The increased SOA mass due to increasing MT emissions is indicated by the upward pointing arrow in the "SOA" column in Table 5. According to Lathière et al. (2005), higher mean temperatures as well as expansion of vegetation zones will cause higher overall MT emissions, resulting in higher SOA mass (Tsigarides and Kanakidou, 2007). Hence, under negligible stress, the consequence of increased MT emissions will be a negative climatic feedback, as already suggested by Kulmala et al. (2004) and corroborated by Spracklen et al. (2008). However, already the presence of more than 10 % of isoprene in a given constitutive mix will suppress particle formation (Kiendler-Scharr et al., 2009). As indicated by downward pointing arrow in the "SOA" column in Table 5, increasing isoprene emissions will thus weaken the negative feedback of MT-SOA.

SIE with high incremental yields and efficiency for particle formation are emitted under biotic stress. Emissions of SQT, phenolic BVOC, or C_{17}-BVOC may appear only episodically and not permanently. Nevertheless, these emissions can last for weeks and with high SOA formation potentials of 20 % or 30 % they may have a substantial impact. As far as known, biotic stress will lead to enhanced SIE and – as was shown here – to increased SOA formation (upward arrows Table 5), unless the stressor induces strong GLV emissions. In cases of strong GLV emissions the yields of SOA formation will be suppressed as indicated by the downward arrow in Table 5.

In few examples we will now apply the classifications in Table 5 to Boreal and Temperate forests considering typical tree species in order to depict possible couplings between stress to plants, SOA formation, and changing climate. The impacts of future stress on particle formation are assessed for the isolated ecosystem. Impacts on net photosynthesis and transpiration will not be considered here. For simplicity we also neglect complications by possible anthropogenic enhancement of biogenic SOA production recently discussed by Spracklen et al. (2011). We furthermore simplify by assuming that the physico-chemical processes leading to particle formation in the atmosphere as well as atmospheric boundary conditions such as OH levels and NO_x concentrations remain unchanged.

For estimation of the sign of possible feedbacks we refer to the relation of increasing SOA production, particle size, and cooling aerosol effects as described in Sect. 4.1. Therefore, if less particulate mass is produced from the BVOC mix either by reduced amounts of emissions or by suppression by isoprene and GLV, we expect a positive feedback. If more SOA mass is produced from increased emissions of MT we expect a negative feedback. Based on these considerations we propose the feedback schemes as shown in Fig. 9.

Regarding the high diversity of ecosystems and their interactions, Fig. 9 can only serve as a first guidance. However, some trends deserve a closer examination. Heat and drought stress can induce negative feedbacks and nota bene a positive feedback in one case. Biotic stress tends to increase overall BVOC emissions and incremental SOA yields, at least for a short (days to weeks) time periods. As long as biotic stress remains below a level that induces strong GLV emissions (or is killing the host) the mix will have a higher capacity to form SOA mass. Therefore we would expect a negative climate feedback if biotic stresses for plants in an ecosystem would increase due to climate warming. Note, that impacts of biotic stress on net photosynthesis and transpiration must still be considered in addition.

Biotic stresses such as insect or pathogen infestation of plants are existing already nowadays. For example, the expansion of tree damage by bark beetles in the Rocky Mountains is and its front range has been linked to climatic change and the associated temperature changes (Bentz et al., 2010; Berg et al., 2012). It is thus likely that BVOC emissions are already influenced by biotic stressors in some regions of the world. Extreme impacts of climate change on top of these can lead to a drop of BVOC emissions induced by biotic stress, such as the observed reaction to the applied heat stress to spruce (Fig. 4). Assuming that biotic stress already exists at some level, the overall effect of future heat and droughts can turn the coupling from a negative to a positive feedback. A key question for assessing the impacts of stress on the complex vegetation–atmosphere–climate interactions under future climate conditions therefore is: are conditions for biotic stressors favored or hindered by occurrence of heat or drought periods?

5 Conclusions

We determined the SOA formation potential of SIE from common trees of Temperate and Boreal forests (Pine, Spruce, Birch, and Beech). SOA mass yields were larger than those due to constitutive MT emissions: 17 ± 1 % for SQT, 20 ± 3 % for MeSa, and 30 ± 4 % for C_{17}-BVOC. In contrast to these SIE classes emitted due to biotic stress, GLV emissions have the potential to decrease SOA mass and number. Increased GLV emissions support positive feedback in case GLV emissions are related to heat, however exert a potential negative feedback when related to drought. Our results clearly indicate that different stress conditions can affect biogenic SOA production: stress induced changes of BVOC emission patterns and strength strongly impact SOA formation causing increased (SQT, MeSa, C_{17}-BVOC) or decreased (GLV) SOA formation.

Our study and consequent considerations strongly suggest the importance of SIE for the existence of feedbacks between climate and vegetation via SOA formation. Biotic stress supports negative feedback and this may be effective already today. But heat and drought can turn the negative feedback proposed by Kulmala et al. (2004) and Goldstein et al. (2009) into a positive feedback in Temperate Forests dominated by *de novo* emitters. Since it is likely that climate change will affect SIE from vegetation, SIE and their SOA formation potential have to be considered in future climate scenarios.

Acknowledgements. The authors acknowledge financial support by the integrated EU projects EUCAARI (Contract No. 036833-2) and PEGASOS (Contract No. 265307). Y. R. acknowledges support from the US-Israel bi-national science foundation (BSF) contract number 2008/146 and support by the Helen and Martin Kimmel Award for Innovative Investigation.

The service charges for this open access publication
have been covered by a Research Centre of the
Helmholtz Association.

References

Albrecht, B. A.: Aerosols, cloud microphysics, and fractional cloudiness, Science, 245, 1227–1230, doi:10.1126/science.245.4923.1227, 1989.

Arimura, G., Huber, D. P. W., and Bohlmann, J.: Forest tent caterpillars (*malacosoma disstria*) induce local and systemic diurnal emissions of terpenoid volatiles in hybrid poplar (*populus trichocarpa x deltoides*): cDNA cloning, functional characterization, and patterns of gene expression of (-)-germacrene d synthase, PtdTPS1, Plant J., 37, 603–616, doi:10.1111/j.1365-313X.2003.01987.x, 2004.

Arneth, A. and Niinemets, Ü.: Induced BVOCS: How to bug our models?, Trends in Plant Science, 15, 118–125, 2010.

Arneth, A., Harrison, S. P., Zaehle, S., Tsigaridis, K., Menon, S., Bartlein, P. J., Feichter, J., Korhola, A., Kulmala, M., O'Donnell, D., Schurgers, G., Sorvari, S., and Vesala, T.: Terrestrial biogeochemical feedbacks in the climate system, Nat. Geosci., 3, 525–532, doi:10.1038/ngeo905, 2010.

Ayres, M. P. and Lombardero, M. J.: Assessing the consequences of global change for forest disturbance from herbivores and pathogens, Sci. Total Environ., 262, 263–286, doi:10.1016/s0048-9697(00)00528-3, 2000.

Bentz, B. J., Regniere, J., Fettig, C. J., Hansen, E. M., Hayes, J. L., Hicke, J. A., Kelsey, R. G., Negron, J. F., and Seybold, S. J.: Climate change and bark beetles of the Western United States and Canada: direct and indirect effects, Bioscience, 60, 602–613, doi:10.1525/bio.2010.60.8.6, 2010.

Berg, A. R., Heald, C. L., Huff Hartz, K. E., Hallar, A. G., Meddens, A. J. H., Hicke, J. A., Lamarque, J.-F., and Tilmes, S.: The impact of bark beetle infestation on monoterpene emissions and secondary organic aerosol formation in Western North America, Atmos. Chem. Phys. Discuss., 12, 29763–29800, doi:10.5194/acpd-12-29763-2012, 2012.

Brilli, F., Barta, C., Fortunati, A., Lerdau, M., Loreto, F., and Centritto, M.: Response of isoprene emission and carbon metabolism to drought in white poplar (*populus alba*) saplings, New Phytol., 175, 244–254, doi:10.1111/j.1469-8137.2007.02094.x, 2007.

Boland, W., Hopke, J., Donath, J., Nuske, J., and Bublitz, F.: Jasmonic acid and coronatin induce odor production in plants, Angew. Chem. Int. Edit., 34, 1600–1602, doi:10.1002/anie.199516001, 1995.

Carslaw, K. S., Boucher, O., Spracklen, D. V., Mann, G. W., Rae, J. G. L., Woodward, S., and Kulmala, M.: A review of natural aerosol interactions and feedbacks within the Earth system, Atmos. Chem. Phys., 10, 1701–1737, doi:10.5194/acp-10-1701-2010, 2010.

Chen, I. C., Hill, J. K., Ohlemuller, R., Roy, D. B., and Thomas, C. D.: Rapid range shifts of species associated with high levels of climate warming, Science, 333, 1024–1026, doi:10.1126/science.1206432, 2011.

Chen, Y., Li, Q. B., Kahn, R. A., Randerson, J. T., and Diner, D. J.: Quantifying aerosol direct radiative effect with multiangle imaging spectroradiometer observations: top-of-atmosphere albedo change by aerosols based on land surface types, J. Geophys. Res., 114, D02109, doi:10.1029/2008jd010754, 2009.

Colquhoun, T. A., Schimmel, B. C. J., Kim, J. Y., Reinhardt, D., Cline, K., and Clark, D. G.: A petunia chorismate mutase specialized for the production of floral volatiles, Plant J., 61, 145–155, doi:10.1111/j.1365-313X.2009.04042.x, 2010.

Croft, K. P. C., Juttner, F., and Slusarenko, A. J.: Volatile products of the lipoxygenase pathway evolved from *phaseolus vulgaris* (L.) leaves inoculated with *pseudomonas syringae* pv *phaseolicola*, Plant Physiol., 101, 13–24, 1993.

Dal Maso, M., Hari, P., and Kulmala, M.: Spring recovery of photosynthesis and atmospheric particle formation, Boreal Environ. Res., 14, 711–721, 2009.

Goldstein, A. H., Koven, C. D., Heald, C. L., and Fung, I. Y.: Biogenic carbon and anthropogenic pollutants combine to form a cooling haze over the southeastern united states, P. Natl. Acad. Sci., 106, 8835–8840, doi:10.1073/pnas.0904128106, 2009.

Gouinguene, S. P., and Turlings, T. C. J.: The effects of abiotic factors on induced volatile emissions in corn plants, Plant Physiol., 129, 1296–1307, doi:10.1104/pp.001941, 2002.

Guenther, A., Hewitt, C. N., Erickson, D., Fall, R., Geron, C., Graedel, T., Harley, P., Klinger, L., Lerdau, M., McKay, W. A., Pierce, T., Scholes, B., Steinbrecher, R., Tallamraju, R., Taylor, J., and Zimmerman, P.: A global model of natural volatile organic compound emissions, J. Geophys. Res., 100, 8873–8892, 1995.

Guenther, A. B., Zimmerman, P. R., Harley, P. C., Monson, R. K., and Fall, R.: Isoprene and monoterpene emission rate variability – model evaluations and sensitivity analyses, J. Geophys. Res., 98, 12609–12617, doi:10.1029/93jd00527, 1993.

Guenther, A. B., Jiang, X., Heald, C. L., Sakulyanontvittaya, T., Duhl, T., Emmons, L. K., and Wang, X.: The Model of Emissions of Gases and Aerosols from Nature version 2.1 (MEGAN2.1): an extended and updated framework for modeling biogenic emissions, Geosci. Model Dev., 5, 1471–1492, doi:10.5194/gmd-5-1471-2012, 2012.

Hamilton, J. F., Lewis, A. C., Carey, T. J., Wenger, J. C., Borrás i Garcia, E., and Muñoz, A.: Reactive oxidation products promote secondary organic aerosol formation from green leaf volatiles, Atmos. Chem. Phys., 9, 3815–3823, doi:10.5194/acp-9-3815-2009, 2009.

Hansen, U. and Seufert, G.: Terpenoid emission from *Citrus sinensis* (L.) OSBECK under drought stress, Phys. Chem. Earth B, 24, 681–687, doi:10.1016/s1464-1909(99)00065-9, 1999.

Hao, L. Q., Romakkaniemi, S., Yli-Pirilä, P., Joutsensaari, J., Kortelainen, A., Kroll, J. H., Miettinen, P., Vaattovaara, P., Tiitta, P., Jaatinen, A., Kajos, M. K., Holopainen, J. K., Heijari, J., Rinne, J., Kulmala, M., Worsnop, D. R., Smith, J. N., and Laaksonen, A.: Mass yields of secondary organic aerosols from the oxidation of α-pinene and real plant emissions, Atmos. Chem. Phys., 11, 1367–1378, doi:10.5194/acp-11-1367-2011, 2011.

Heald, C. L., Henze, D. K., Horowitz, L. W., Feddema, J., Lamarque, J. F., Guenther, A., Hess, P. G., Vitt, F., Seinfeld, J. H., Goldstein, A. H., and Fung, I.: Predicted change in global secondary organic aerosol concentrations in response to future climate, emissions, and land use change, J. Geophys. Res., 113, D05211, doi:10.1029/2007jd009092, 2008.

Heiden, A. C., Hoffmann, T., Kahl, J., Kley, D., Klockow, D., Langebartels, C., Mehlhorn, H., Sandermann, H., Schraudner, M., Schuh, G., and Wildt, J.: Emission of volatile organic compounds from ozone-exposed plants, Ecol. Appl., 9, 1160–1167, 1999.

Heiden, A. C., Kobel, K., Langebartels, C., Schuh-Thomas, G., and Wildt, J.: Emissions of oxygenated volatile organic compounds from plants – Part I: Emissions from lipoxygenase activity, J. Atmos. Chem., 45, 143–172, 2003.

Hicke, J. A., Allen, C. D., Desai, A. R., Dietze, M. C., Hall, R. J., Hogg, E. H., Kashian, D. M., Moore, D., Raffa, K. F., Sturrock, R. N., and Vogelmann, J.: Effects of biotic disturbances on forest carbon cycling in the United States and Canada, Glob. Change Biol., 18, 7–34, doi:10.1111/j.1365-2486.2011.02543.x, 2012

Hopke, J., Donath, J., Blechert, S., and Boland, W.: Herbivore-induced volatiles – the emission of acyclic homoterpenes from leaves of *Phaseolus lunatus* and *Zea mays* can be triggered by a β-glucosidase and jasmonic acid, FEBS Lett., 352, 146–150, doi:10.1016/0014-5793(94)00948-1, 1994.

Joó, E., Dewulf, J., Amelynck, C., Schoon, N., Pokorska, O., Šimpraga, M., Steppe, K., Aubinet, M., and Van Langenhove, H.: Constitutive versus heat and biotic stress induced BVOC emissions in *Pseudotsuga menziesii*, Atmos. Environ., 45, 3655–3662, doi:10.1016/j.atmosenv.2011.04.048, 2011.

Joutsensaari, J., Loivamäki, M., Vuorinen, T., Miettinen, P., Nerg, A.-M., Holopainen, J. K., and Laaksonen, A.: Nanoparticle formation by ozonolysis of inducible plant volatiles, Atmos. Chem. Phys., 5, 1489–1495, doi:10.5194/acp-5-1489-2005, 2005.

Kaufman, Y. J., Tanre, D., and Boucher, O.: A satellite view of aerosols in the climate system, Nature, 419, 215–223, doi:10.1038/nature01091, 2002.

Kerminen, V. M., Lihavainen, H., Komppula, M., Viisanen, Y., and Kulmala, M.: Direct observational evidence linking atmospheric aerosol formation and cloud droplet activation, Geophys. Res. Lett., 32, L14803, doi:10.11029/12005GL023130, 2005.

Kesselmeier, J. and Staudt, M.: Biogenic volatile organic compounds (VOC): an overview on emission, physiology and ecology, J. Atmos. Chem., 33, 23–88, doi:10.1023/a:1006127516791, 1999.

Kiendler-Scharr, A., Wildt, J., Dal Maso, M., Hohaus, T., Kleist, E., Mentel, T. F., Tillmann, R., Uerlings, R., Schurr, U., and Wahner, A.: New particle formation in forests inhibited by isoprene emissions, Nature, 461, 381–384, doi:10.1038/nature08292, 2009.

Kiendler-Scharr, A., Andres, S., Bachner, M., Behnke, K., Broch, S., Hofzumahaus, A., Holland, F., Kleist, E., Mentel, T. F., Rubach, F., Springer, M., Steitz, B., Tillmann, R., Wahner, A., Schnitzler, J.-P., and Wildt, J.: Isoprene in poplar emissions: effects on new particle formation and OH concentrations, Atmos. Chem. Phys., 12, 1021–1030, doi:10.5194/acp-12-1021-2012, 2012.

Kleist, E., Mentel, T. F., Andres, S., Bohne, A., Folkers, A., Kiendler-Scharr, A., Rudich, Y., Springer, M., Tillmann, R., and Wildt, J.: Irreversible impacts of heat on the emissions of monoterpenes, sesquiterpenes, phenolic BVOC and green leaf volatiles from several tree species, Biogeosciences, 9, 5111–5123, doi:10.5194/bg-9-5111-2012, 2012.

Kulmala, M., Suni, T., Lehtinen, K. E. J., Dal Maso, M., Boy, M., Reissell, A., Rannik, Ü., Aalto, P., Keronen, P., Hakola, H., Bäck, J., Hoffmann, T., Vesala, T., and Hari, P.: A new feedback mechanism linking forests, aerosols, and climate, Atmos. Chem. Phys., 4, 557–562, doi:10.5194/acp-4-557-2004, 2004.

Lang-Yona, N., Rudich, Y., Mentel, Th. F., Bohne, A., Buchholz, A., Kiendler-Scharr, A., Kleist, E., Spindler, C., Tillmann, R., and Wildt, J.: The chemical and microphysical properties of secondary organic aerosols from Holm Oak emissions, Atmos. Chem. Phys., 10, 7253–7265, doi:10.5194/acp-10-7253-2010, 2010.

Laothawornkitkul, J., Taylor, J. E., Paul, N. D., and Hewitt, C. N.: Biogenic volatile organic compounds in the earth system, New Phytol., 183, 27–51, doi:10.1111/j.1469-8137.2009.02859.x, 2009.

Lathière, J., Hauglustaine, D. A., De Noblet-Ducoudré, N., Krinner, G., and Folberth, G. A.: Past and future changes in biogenic volatile organic compound emissions simulated with a global dynamic vegetation model, Geophys. Res. Lett., 32, L20818, doi:10.1029/2005GL024164, 2005.

Lohmann, U. and Feichter, J.: Global indirect aerosol effects: a review, Atmos. Chem. Phys., 5, 715–737, doi:10.5194/acp-5-715-2005, 2005.

Loreto, F. and Schnitzler, J. P.: Abiotic stresses and induced BVOCs, Trends Plant Sci., 15, 154–166, doi:10.1016/j.tplants.2009.12.006, 2010.

Maes, K. and Debergh, P. C.: Volatiles emitted from in vitro grown tomato shoots during abiotic and biotic stress, Plant Cell Tiss. Org., 75, 73–78, doi:10.1023/a:1024650006740, 2003.

Mentel, Th. F., Wildt, J., Kiendler-Scharr, A., Kleist, E., Tillmann, R., Dal Maso, M., Fisseha, R., Hohaus, Th., Spahn, H., Uerlings, R., Wegener, R., Griffiths, P. T., Dinar, E., Rudich, Y., and Wahner, A.: Photochemical production of aerosols from real plant emissions, Atmos. Chem. Phys., 9, 4387–4406, doi:10.5194/acp-9-4387-2009, 2009.

Nazzi, F., Milani, N., and Della Vedova, G.: (Z)-8-heptadecene from infested cells reduces the reproduction of *varroa destructor* under laboratory conditions, J. Chem. Ecol., 28, 2181–2190, doi:10.1023/a:1021041130593, 2002.

Niinemets, Ü., Arneth, A., Kuhn, U., Monson, R. K., Peñuelas, J., and Staudt, M.: The emission factor of volatile isoprenoids: stress, acclimation, and developmental responses, Biogeosciences, 7, 2203–2223, doi:10.5194/bg-7-2203-2010, 2010.

Ormeño, E., Mévy, J. P., Vila, B., Bousquet-Mélou, A., Greff, S., Bonin, G., and Fernandez, C.: Water deficit stress induces different monoterpene and sesquiterpene emission changes in mediterranean species. Relationship between terpene emissions and plant water potential, Chemosphere, 67, 276–284, doi:10.1016/j.chemosphere.2006.10.029, 2007.

Peñuelas, J. and Staudt, M.: BVOCs and global change, Trends Plant Sci., 15, 133–144, doi:10.1016/j.tplants.2009.12.005, 2010.

Pilinis, C., Pandis, S. N., and Seinfeld, J. H.: Sensitivity of direct climate forcing by atmospheric aerosols to aerosol-size and composition, J. Geophys. Res., 100, 18739–18754, doi:10.1029/95jd02119, 1995.

Quaas, J., Ming, Y., Menon, S., Takemura, T., Wang, M., Penner, J. E., Gettelman, A., Lohmann, U., Bellouin, N., Boucher, O., Sayer, A. M., Thomas, G. E., McComiskey, A., Feingold, G., Hoose, C., Kristjánsson, J. E., Liu, X., Balkanski, Y., Donner, L. J., Ginoux, P. A., Stier, P., Grandey, B., Feichter, J., Sednev, I., Bauer, S. E., Koch, D., Grainger, R. G., Kirkevåg, A., Iversen, T., Seland, Ø., Easter, R., Ghan, S. J., Rasch, P. J., Morrison, H., Lamarque, J.-F., Iacono, M. J., Kinne, S., and Schulz, M.: Aerosol indirect effects – general circulation model intercomparison and evaluation with satellite data, Atmos. Chem. Phys., 9, 8697–8717, doi:10.5194/acp-9-8697-2009, 2009.

Rasulov, B., Hüve, K., Bichele, I., Laisk, A., and Niinemets, Ü.: Temperature response of isoprene emission in vivo reflects a combined effect of substrate limitations and isoprene synthase activity: a kinetic analysis, Plant Physiol., 154, 1558–1570, doi:10.1104/pp.110.162081, 2010.

Riipinen, I., Pierce, J. R., Yli-Juuti, T., Nieminen, T., Häkkinen, S., Ehn, M., Junninen, H., Lehtipalo, K., Petäjä, T., Slowik, J., Chang, R., Shantz, N. C., Abbatt, J., Leaitch, W. R., Kerminen, V.-M., Worsnop, D. R., Pandis, S. N., Donahue, N. M., and Kulmala, M.: Organic condensation: a vital link connecting aerosol formation to cloud condensation nuclei (CCN) concentrations, Atmos. Chem. Phys., 11, 3865–3878, doi:10.5194/acp-11-3865-2011, 2011.

Schuh, G., Heiden, A. C., Hoffmann, T., Kahl, J., Rockel, P., Rudolph, J., and Wildt, J.: Emissions of volatile organic compounds from sunflower and beech: dependence on temperature and light intensity, J. Atmos. Chem., 27, 291–318, 1997.

Šimpraga, M., Verbeeck, H., Demarcke, M., Joó, E., Pokorska, O., Amelynck, C., Schoon, N., Dewulf, J., Van Langenhove, H., Heinesch, B., Aubinet, M., Laffineur, Q., Müller, J. F., and Steppe, K.: Clear link between drought stress, photosynthesis and biogenic volatile organic compounds in *Fagus sylvatica* L., Atmos. Environ., 45, 5254–5259, doi:10.1016/j.atmosenv.2011.06.075, 2011.

Sitch, S., Cox, P. M., Collins, W. J., and Huntingford, C.: Indirect radiative forcing of climate change through ozone effects on the land-carbon sink, Nature, 448, 791–794, doi:10.1038/nature06059, 2007.

Spracklen, D. V., Bonn, B., and Carslaw, K. S.: Boreal forests, aerosols and the impacts on clouds and climate, Philos. T. R. Soc. A, 366, 4613–4626, doi:10.1098/rsta.2008.0201, 2008.

Spracklen, D. V., Jimenez, J. L., Carslaw, K. S., Worsnop, D. R., Evans, M. J., Mann, G. W., Zhang, Q., Canagaratna, M. R., Allan, J., Coe, H., McFiggans, G., Rap, A., and Forster, P.: Aerosol mass spectrometer constraint on the global secondary organic aerosol budget, Atmos. Chem. Phys., 11, 12109–12136, doi:10.5194/acp-11-12109-2011, 2011.

Sturrock, R. N., Frankel, S. J., Brown, A. V., Hennon, P. E., Kliejunas, J. T., Lewis, K. J., Worrall, J. J., and Woods, A. J.: Climate change and forest diseases, Plant Pathol., 60, 133–149, doi:10.1111/j.1365-3059.2010.02406.x, 2011.

Trenberth, K. E., Jones, P. D., Ambenje, P., Bojariu, R., Easterling, D., Klein Tank, A., Parker, D., Rahimzadeh, F., Renwick, J. A., Rusticucci, M., Soden, B., and Zhai, P.: Observations: Surface and atmospheric climate change, in: Climate Change 2007: the Physical Science Basis, Contribution of working group I to the fourth assessment report of the intergovernmental panel on climate change, edited by: Solomon, S., Qin, D., Manning, M., Chen, Z., Marquis, M., Averyt, K. B., Tignor, M., and Miller, H. L., Cambridge University Press, Cambridge, UK and New York, NY, USA, 235–336, 2007.

Tsigaridis, K. and Kanakidou, M.: Secondary organic aerosol importance in the future atmosphere, Atmos. Environ., 41, 4682–4692, 2007.

Tunved, P., Hansson, H. C., Kerminen, V. M., Strom, J., Dal Maso, M., Lihavainen, H., Viisanen, Y., Aalto, P. P., Komppula, M., and Kulmala, M.: High natural aerosol loading over Boreal forests, Science, 312, 261–263, 2006.

Tunved, P., Strom, J., Kulmala, M., Kerminen, V. M., Dal Maso, M., Svenningson, B., Lunder, C., and Hansson, H. C.: The natural aerosol over northern europe and its relation to anthropogenic emissions – implications of important climate feedbacks, Tellus B, 60, 473–484, 2008.

Twomey, S.: Influence of pollution on shortwave albedo of clouds, J. Atmos. Sci., 34, 1149–1152, doi:10.1175/1520-0469(1977)034<1149:tiopot>2.0.co;2, 1977.

Table 1. Overview over experiments with trees and control experiments.

No	Purpose of experiment	Plants used	Remarks
1	Impact of biotic SIE on SOA formation	Silver birch, Scots pine, Norway spruce	High degree of aphid infestation of spruce
1c	Contribution of MeSa to SOA formation	Control experiment with BVOC from diffusion source	MeSa addition to α-pinene
2	Impact of heat stress on SOA formation from biotic SIE	Norway spruce	High degree of aphid infestation
3	Impact of drought stress on SOA formation (interaction of GLV emissions and emissions of C_{17}-BVOC)	Silver birch, European beech, Norway spruce	Spruce infested by *cinara pilicornis*
3c	Impact of GLV on SOA formation	Control experiment with BVOC from diffusion source	(Z)-3-hexenol addition to α-pinene

Table 2. Plant chamber temperatures and MT/SQT concentration ratios ([µg m^{-3}]/[µg m^{-3}]) during Experiment #2 with Norway spruce. Days relative to the day of heat stress application at day 0. Note that the needle temperature was about 4 °C higher than the listed plant chamber temperature during periods of illumination (compare Kleist et al., 2012).

Day	−5	−4	−3	−2	−1	0	1	2	3	4	5
T [°C]	20	15	15	20	25	35	30	20	20	20	20
MT/SQT	0.4	0.27	0.32	0.49	1.7	19	15	> 100	66	81	> 100

ACPD
13, 7463–7502, 2013

Table 3. Major BVOC emitted from the set of plants used in the Experiment #1 (data is for day 5 in Fig. 1). BVOC with concentrations above 0.1 $\mu g\,m^{-3}$ are listed explicitly. Concentrations listed for the sum of BVOC classes include also BVOC with concentrations below 0.1 $\mu g\,m^{-3}$.

BVOC	Class	Conc. [$\mu g\,m^{-3}$]	Contribution [%]
Isoprene	C5	0.71	0.4
(Z)-3-hexenol	GLV	0.16	0.09
(Z)-3-hexenylacetate	GLV	1.5	0.8
Sum green leaf volatiles	GLV	2.01	1.1
α-pinene	MT	1.05	0.57
Camphene	MT	0.21	0.11
Sabinene	MT	0.14	0.08
Myrcene	MT	0.77	0.42
β-pinene	MT	0.16	0.09
Δ^3carene	MT	0.68	0.37
Limonene	MT	0.53	0.29
β-phellandrene + cis-ocimene[a]	MT	0.28	0.15
(E)-β-ocimene	MT	4.57	2.5
Terpinolene	MT	3.22	1.7
Alloocimene	MT	2.15	1.2
1,8-cineole	MT	0.77	0.4
DMNT[b]	MT °	2.07	1.1
Sum monoterpenes	MT	17.9	9.7
(E)-β-caryophyllene[c]	SQT	0.11	0.06
(E)-α-bergamontene	SQT	0.13	0.07
(E)-β-farnesene	SQT	65.5	35.5
α-curcumene[c]	SQT	0.14	0.08
(E)-farnesene[c]	SQT	0.26	0.14
β-bisabolene	SQT	0.18	0.1
(E,E)-α-farnesene	SQT	30.1	16.3
Δ-cadinene	SQT	0.17	0.09
(Z)-α-bisabolene	SQT	4.37	2.4
Sum sesquiterpenes	SQT	104	56.3
MeSa	Phen.	48	26
Benzoic acid methyl ester	Phen.	1.9	1.0
Benzyl benzoate	Phen.	0.5	0.27
Sum phenolic BVOC	Phen.	59.9	32.4
Other BVOC[d]		0.22	0.1

[a] Treated together because of a strong overlap in chromatographic peaks.

[b] DMNT = (Z)-4,8-dimethyl-1,3,7-nonatriene = homoterpene (C_{11}) but for simplification added to MT.

[c] Only tentative identification with match quality below 95 % or overlap with other chromatographic peaks.

[d] Includes compounds with so far unknown biosynthesis as nonanal, decanal etc.

Table 4. Overview over incremental SOA mass yields observed for SIE in this study and MT emissions in the literature.

Name	BVOC source	Action	Major BVOC	Incremental Mass yield
Exp1	Stand	Aphid infestation	SQT/MeSa	22 ± 2 %
Exp1c	Diff. source		MeSa	20 ± 3 %
Exp2	Spruce	Aphid infestation and heat	SQT	17 ± 1 %
Exp3	Stand	*Cinara pilicornis* infestation and drought	C_{17}-BVOC GLV	33 ± 6 %
Exp3c	Diff. source		α-pinene + Z3-hexenol	
[a]	Grey poplar	Ozone pulse	SQT/MeSa	20 ± 6 %
[b]	Pine	None	MT 80 %	5.3 ± 0.5 %
[b]	Spruce	None	MT 90 %	4.2 ± 0.7 %
[b]	Diff. source		α-pinene	5.2 ± 0.5 %
[c]	Holm Oak	Heat 25–35 °C	MT	6.0 ± 0.6 %
[d]	Pine/Spruce	None	MT	3–11 %

[a] Kiendler-Scharr et al. (2012).
[b] Mentel et al. (2009).
[c] Lang-Yona et al. (2010).
[d] Hao et al. (2011).

Table 5. BVOC emissions used for estimating impacts of stress induced emissions on SOA formation. Type: Const = constitutive emissions, SIE = stress induced emissions. The SOA column gives the effect of emissions on BSOA assuming increase in emission strengths of the respective BVOC group. The arrows in columns biotic, heat and drought indicate expected trends for the emissions of the respective BVOC group in case of biotic, heat, and drought stress, respectively.

BVOC group	Type	SOA	Biotic	Heat	Drought
MT emissions from pools	Const.	↑	↑[a]	↑[g]	*
MT *de novo* emissions	Const.	↑	↑[b,c]	↓[g]	↓[j,k]
Isoprene	Const.	↓	↑↓[d]	↓[h,i]	↓[k,l]
SQT/*de novo*	SIE	↑	↑[e,f,g]	↓[g]	↓[m,n]
phenolic BVOC	SIE	↑	↑[f,g]	↓[g]	*
GLV	SIE	↓	↑	↑[g]	↑[j]
C_{17}-BVOC	SIE	↑	↑	*	*

[*] either low direct stress impacts or not described in literature.
[a] Niinemets et al. (2010).
[b] Maes and Debergh (2003).
[c] Arimura et al. (2004).
[d] Arneth and Niinemets (2010).
[e] Boland et al. (1995).
[f] Joó et al. (2011).
[g] Kleist et al. (2012).
[h] Guenther et al. (1993).
[i] Rasulov et al. (2010).
[j] Šimpraga et al. (2011).
[k] Laothawornkitkul et al. (2009).
[l] Brilli et al. (2007).
[m] Hansen and Seufert (1999).
[n] Ormeño et al. (2007).

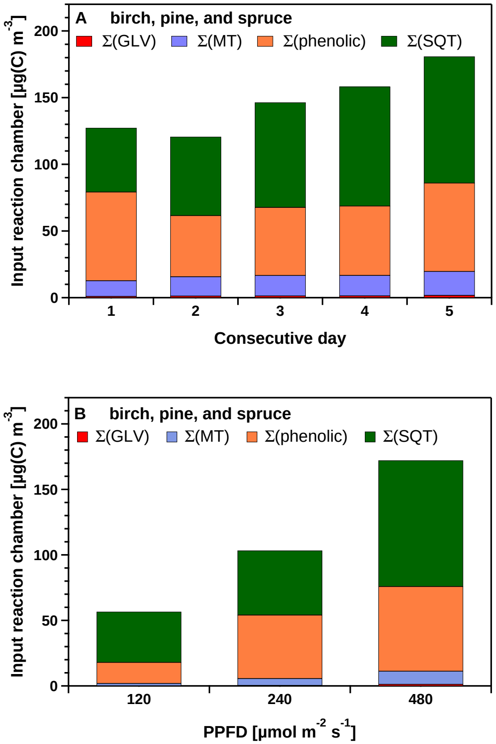

Fig. 1. BVOC concentrations at the inlet of the reaction chamber determined in Experiment #1. Concentrations were averaged for 4 h before particle formation was induced in the reaction chamber. GLV = green leaf volatiles, mainly C_6-alcohols and -aldehydes with significant emissions only at day 5, MT = monoterpenes, phenolic = phenolic BVOC originating downstream of the shikimate pathway, SQT = sesquiterpenes. **(A)** At constant PPFD = 480 µmol m^{-2} s^{-1} and constant plant chamber temperature = 15 °C, during a measurement period of five consecutive days. **(B)** At different PPFD and constant plant chamber temperature = 15 ± 0.5 °C. Note that the pattern depicted for PPFD = 480 µmol m^{-2} s^{-1} is not included in **(A)**.

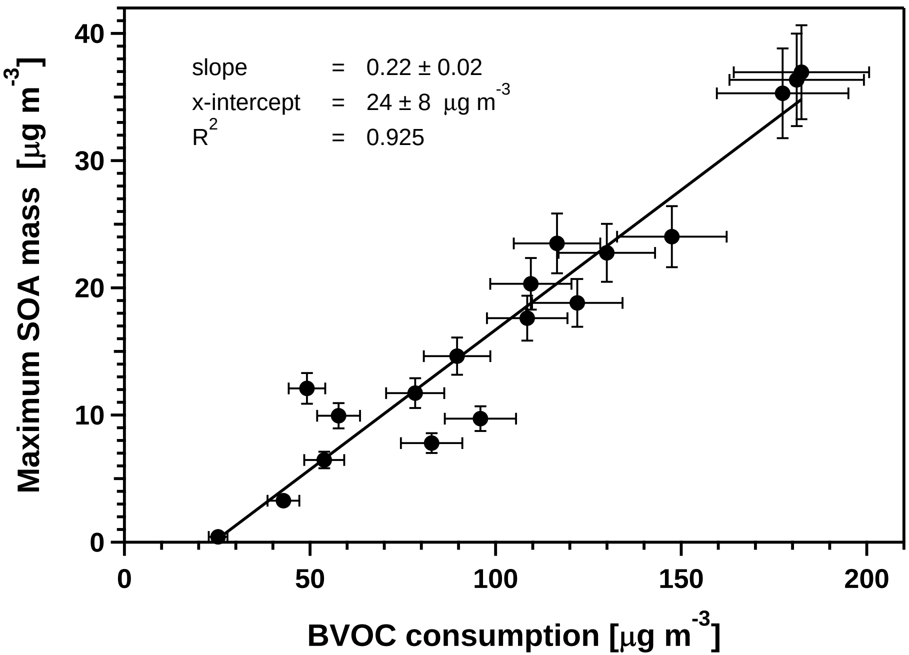

Fig. 2. Maximum SOA mass produced through OH oxidation of BVOC emitted from a birch, a pine and a spruce, the latter infested by aphids (Experiment #1). The linear regression line indicates an incremental yield of 22 ± 2 %. The error bars represent relative errors of ±5 % for the SMPS based SOA mass and ±10 % for the BVOC consumption according to GC calibration errors.

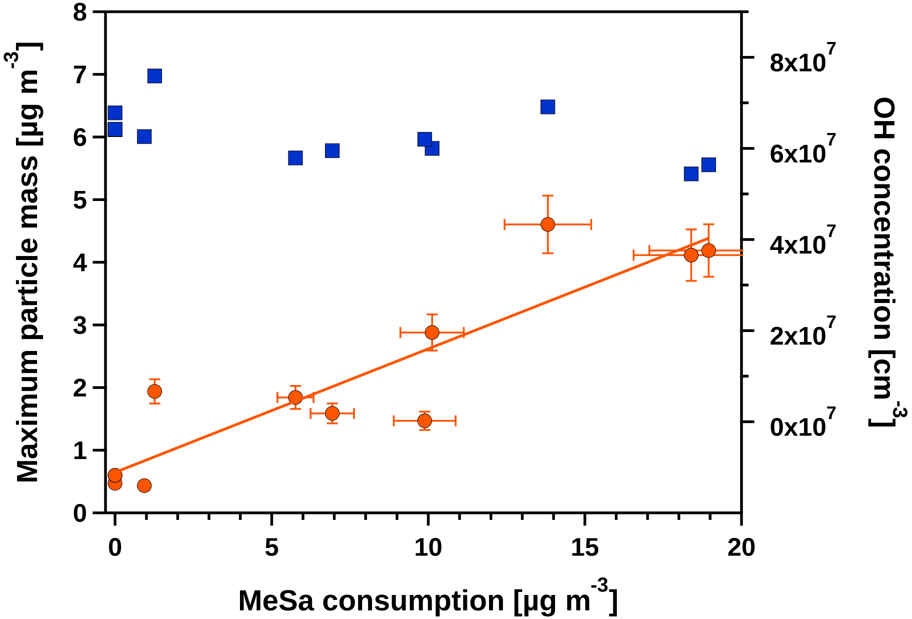

Fig. 3. Maximum SOA mass (orange circles, left scale) and OH concentrations (blue squares, right scale) upon addition of up to 55 µg m^{-3} of MeSa to the reaction chamber in Experiment #1c. The α-pinene concentration was held constant at 27 ± 3 µg m^{-3}. The line shows the result of linear regression analysis giving the yield of 20 ± 3 % (R^2 = 0.83).

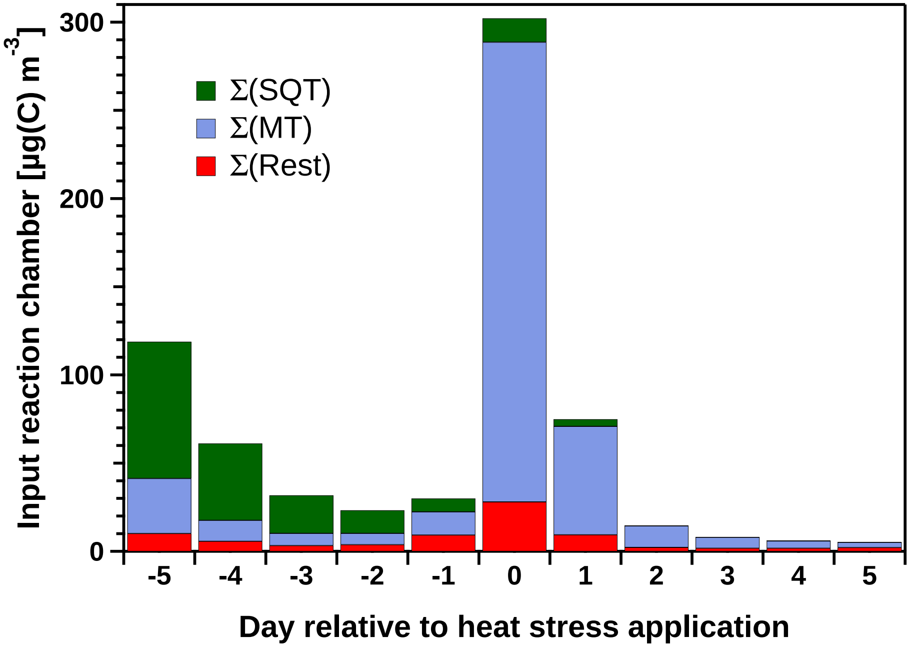

Fig. 4. BVOC concentrations of Experiment #2 at the inlet of the reaction chamber as determined for the insect infested spruce before, during and after heat stress application (35 °C on day 0 and 30 °C on day 1). Data are the mean of 4 h before particle formation was induced in the reaction chamber. SQT = sesquiterpenes, MT = monoterpenes, Rest = phenolic BVOC, GLV, and isoprene.

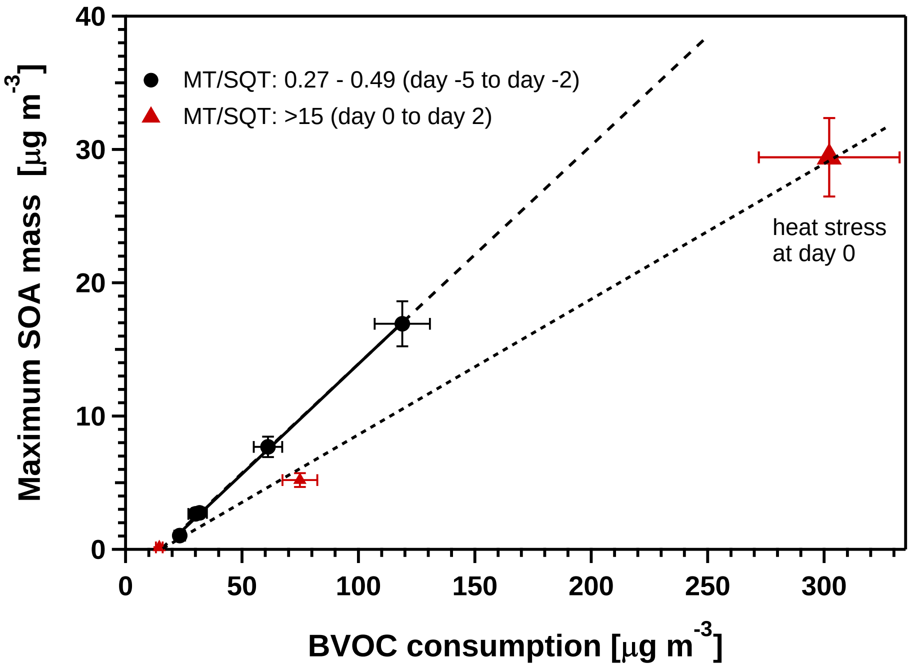

Fig. 5. Maximum SOA mass produced by OH oxidation of BVOC emitted from spruce in Experiment #2. Circles represent the data points obtained at MT/SQT ratios of 0.27–0.49 [$\mu g\,m^{-3}/\mu g\,m^{-3}$] before application of the heat stress (compare Table 2). The solid line shows the result of linear regression analysis giving the yield 17 ± 1 % (x-intercept = 16 ± 1 $\mu g\,m^{-3}$, $R^2 = 0.999$). The large red triangle shows the data point obtained during heat stress application at day 0 with a MT/SQT ratio of 19 [$\mu g\,m^{-3}/\mu g\,m^{-3}$]. The dotted line (slope 0.088 ± 0.002, $R^2 = 0.96$) is calculated using the data of day 0 to day 2 with MT/SQT > 15 (compare Table 2). Dashed extrapolation is given for better comparison of the incremental mass yields for both cases.

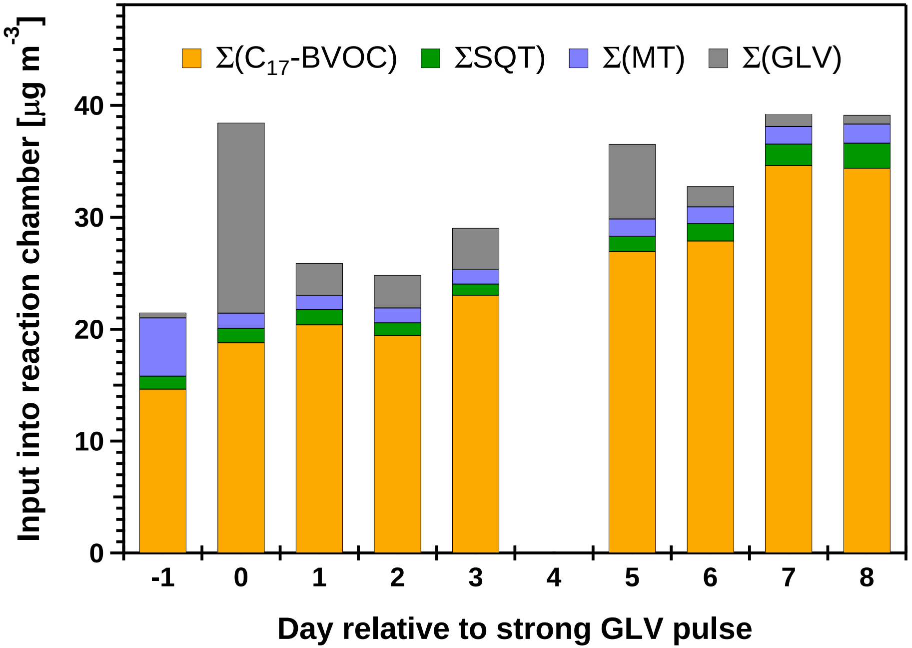

Fig. 6. BVOC pattern in Experiment #3 measured before, during and after a GLV emission pulse. Day 4 is missing because of an instrument failure.

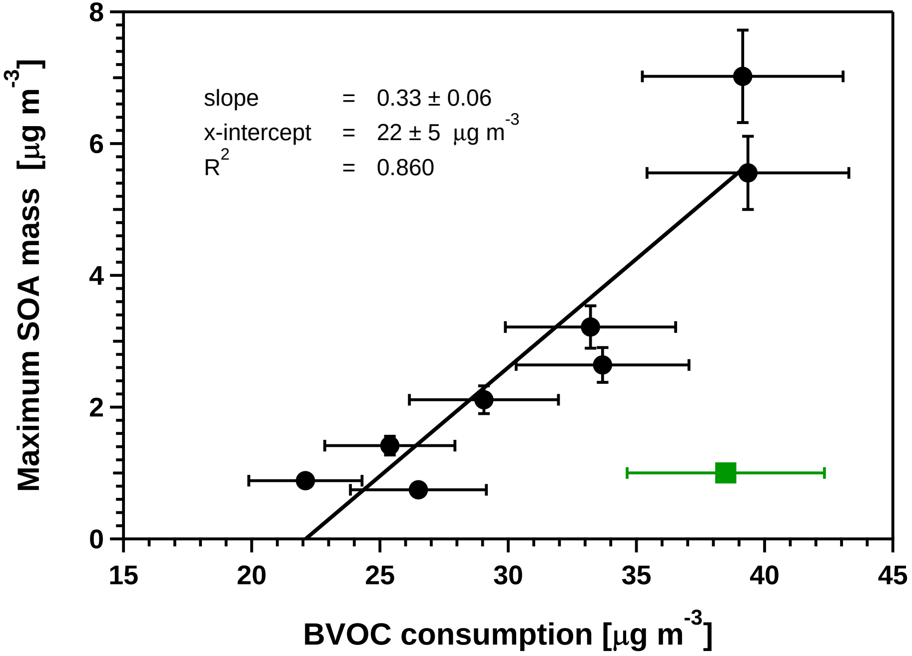

Fig. 7. Maximum SOA mass versus consumption of C_{17}-BVOC dominated emissions in Experiment #3. Black circles: data obtained at low contribution of GLV. Green square data point obtained on day 0 at high GLV emissions (see Fig. 6).

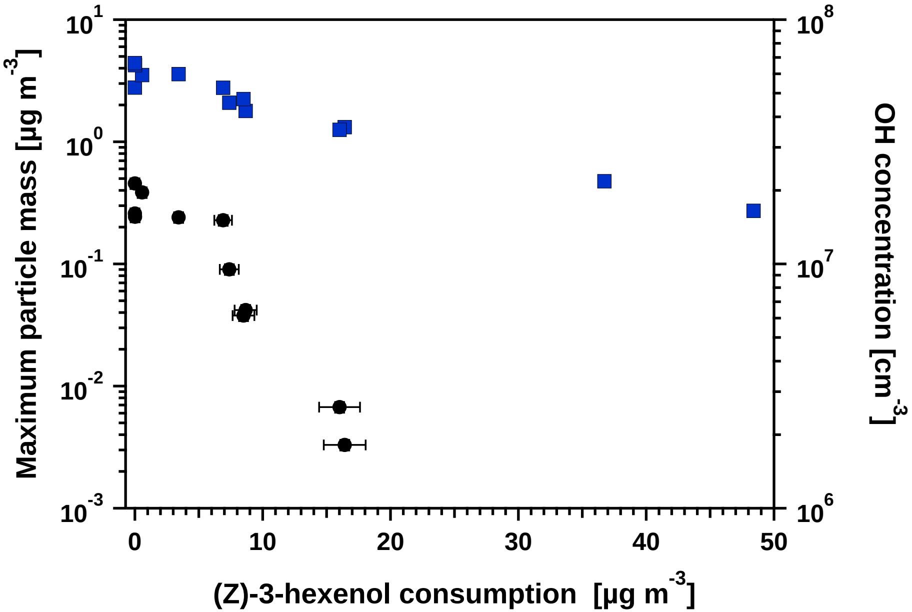

Fig. 8. Maximum particle mass (black circles, left scale) and OH concentrations (blue squares, right scale) upon addition of up to 48 µg m^{-3} of (*Z*)-3-hexenol to the reaction chamber filled with 43 ± 4 µg m^{-3} α-pinene. Above 17 µg m^{-3} (~ 6 ppb) of (Z)-3-hexenol, no particle formation from α-pinene oxidation was observed. Note logarithmic scales on both y-axes.

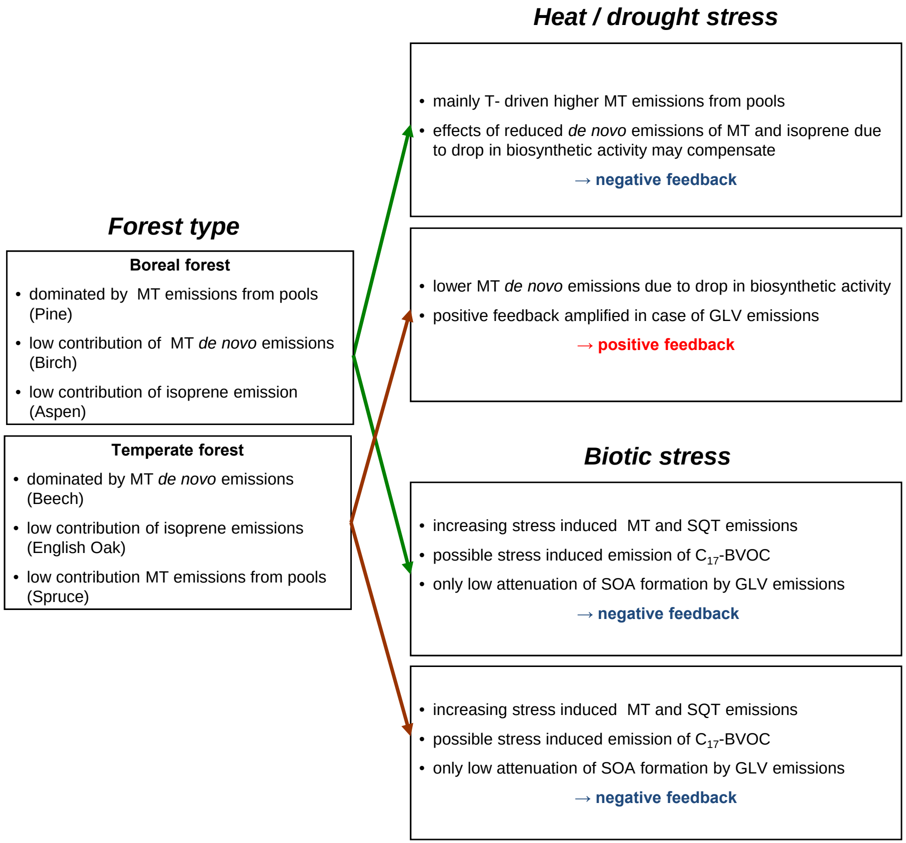

Forest type

Boreal forest

- dominated by MT emissions from pools (Pine)
- low contribution of MT *de novo* emissions (Birch)
- low contribution of isoprene emission (Aspen)

Temperate forest

- dominated by MT *de novo* emissions (Beech)
- low contribution of isoprene emissions (English Oak)
- low contribution MT emissions from pools (Spruce)

Heat / drought stress

- mainly T- driven higher MT emissions from pools
- effects of reduced *de novo* emissions of MT and isoprene due to drop in biosynthetic activity may compensate

→ **negative feedback**

- lower MT *de novo* emissions due to drop in biosynthetic activity
- positive feedback amplified in case of GLV emissions

→ **positive feedback**

Biotic stress

- increasing stress induced MT and SQT emissions
- possible stress induced emission of C_{17}-BVOC
- only low attenuation of SOA formation by GLV emissions

→ **negative feedback**

- increasing stress induced MT and SQT emissions
- possible stress induced emission of C_{17}-BVOC
- only low attenuation of SOA formation by GLV emissions

→ **negative feedback**

Fig. 9. Estimated feedbacks of stress to Temperate and Boreal forest. As negative feedback we understand that enhanced SOA formation and related direct and indirect effects counteract heat and drought. In case of positive feedback the reduced SOA formation enhances effects of heat and drought. For biotic stress we refer to the case that heat and drought increase the chance of pathogen and herbivore attack.